Spectrochimica Acta Part A: Molecular and Biomolecular Spectroscopy 285 (2023) 121901

Contents lists available at ScienceDirect

Spectrochimica Acta Part A:
Molecular and Biomolecular Spectroscopy

journal homepage: www.journals.elsevier.com/spectrochimica-acta-part-a-molecular-and-biomolecular-spectroscopy

Structure and IR spectroscopic properties of complexes of 1,2,4-triazole and 3-amino-1,2,4-triazole with dinitrogen isolated in solid argon

K. Mucha, M. Pagacz-Kostrzewa, J. Krupa, M. Wierzejewska *

Faculty of Chemistry, University of Wrocław, F. Joliot-Curie 14, 50-383 Wrocław, Poland

HIGHLIGHTS

- Complexes formed between triazoles and dinitrogen identified in solid argon.
- Structure of complexes determined by quantum-chemical calculations.
- Triazoles interact with N_2 through hydrogen bond or Van der Waals interactions.
- For 1,2,4-triazole-N_2 multiple trapping sites in argon matrix are present.

GRAPHICAL ABSTRACT

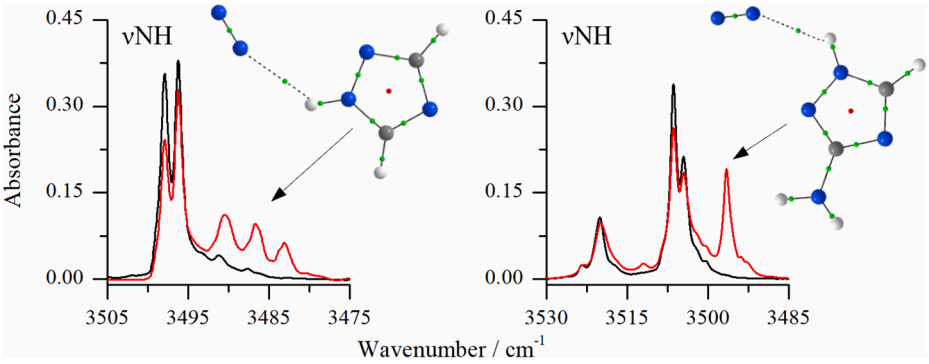

ARTICLE INFO

Keywords:
Azole
Hydrogen bond
van der Waals interaction
Matrices
MP2
DFT

ABSTRACT

Complexes of 1,2,4-triazole (TR) and 3-amino-1,2,4-triazole (AT) with N_2 were studied computationally employing MP2 and B3LYPD3 methods and experimentally by FTIR matrix isolation technique. The results show that both triazoles interact specifically with dinitrogen in several different ways. For the 1:1 complexes of 1,2,4-triazole five stable minima were located on the potential energy surface. The most stable of them comprises a weak hydrogen bond formed between the NH group of the ring and the lone pair of the nitrogen molecule. The second most stable structure is bound by the N···π bond formed between one of the N atoms of the N_2 molecule and the triazole ring. Three other complexes are stabilized by the C-H···N and N···N van der Waals interactions. In the case of 3-amino-1,2,4-triazole, the two most stable dinitrogen complexes are analogous to those found for the 1,2,4-triazole and involve N-H···N and N···π bonds. In other structures amino or CH groups act as proton donors to the N_2 molecule. The N···N van der Waals interactions are also present. The analysis of the infrared spectra of low temperature matrices containing TR or AT and dinitrogen indicates that in both systems mostly 1:1 hydrogen-bonded complexes with the NH group interacting with N_2 are present in solid argon.

* Corresponding author.
E-mail address: maria.wierzejewska@chem.uni.wroc.pl (M. Wierzejewska).

https://doi.org/10.1016/j.saa.2022.121901
Received 16 May 2022; Received in revised form 7 September 2022; Accepted 14 September 2022
Available online 23 September 2022

1. Introduction

Weak intermolecular interactions are of importance in many fields such as biochemistry, medicine or atmospheric chemistry. Matrix isolation technique coupled with infrared spectroscopy is very often used for this type of research. Among the most often studied weakly bound complexes are those containing N_2 molecules. Dinitrogen, the most abundant component of the Earth's atmosphere, is considered to be chemically inert. However, small amounts of N_2, present in the matrix, can lead to considerable changes in the vibrational spectra of the studied molecules. Complexes of N_2 with a number of small molecules with proton donor groups have been extensively studied and the hydrogen bond interaction between the acidic A-H moiety and dinitrogen was identified. Traditional hydrogen bonding with the red wavenumber shifts of the A-H stretching mode upon complexation was found for N_2 complexes with HF [1,2], HCl [3], H_2O [4,5], alcohols [6,7], HCOOH [8,9], HONO [10], HNO_3 [11], CF_3COOH [12], H_2SO_4 [13], HNCS [14], HNCO [15], formaldoxime [16], formohydroxamic acid HCONHOH [17], methylformamide [18], glycolic acid [19,20], phenol [21], pyrrole [22] and others. Several examples of the blue shifted hydrogen bonds have been also reported for complexes of N,N-dimethylformamide [23], chloroform [24] and difluoromethane [25]. Spectroscopic properties of interesting complexes of the noble gas hydrides with dinitrogen have been reported for HXeCl···N_2, HXeBr···N_2 [26], HArF···N_2, HKrF···N_2, HKrCl···N_2 [27] as well as the interaction of the $(NgHNg)^+$ cations (Ng = Ar and Kr) with N_2 has been studied [28]. Several papers on non-hydrogen bonded complexes formed between dinitrogen and various small molecules such as dichlorosilylene $SiCl_2$ [29], silylene SiH_2 [30] or CO_2 [31] were also published. For the latter species interaction was classified to be driven by donor–acceptor or van der Waals forces.

There is a number of studies reported, both experimental and theoretical, on complexes of dinitrogen with benzene and its derivatives [21,32–38]. For the 1:1 phenol-N_2 complex two different minima were located: the planar H-bonded complex with the O-H···N bridge and the π complex with the dinitrogen molecule situated above the center of the aromatic ring. According to Cao et al. [21] the calculated difference of interaction energies between H-bonded and the π structures was found to be, depending on the level of theory, from 0.3 to 1.0 kcal mol^{-1} and energies for both structures were almost the same at MP4/aug-cc-pVTZ (about −2.5 kcal mol^{-1}). Experimentally, only H-bonded complex was identified in a neon matrix with the OH stretching vibration red shifted by 9.2 cm^{-1} relative to the phenol monomer [21]. The papers on the interaction of N_2 with heterocyclic compounds are less frequently published [22,39]. Recently, interaction between pyrrole and dinitrogen has been studied by FTIR spectroscopy in supersonic jet expansions and in low temperature matrices as well as theoretically at the B3LYP-D3(BJ)/aVTZ level of computation [22]. The main goal of this work was to follow the NH stretching shift upon stepwise dinitrogen complexation in neon and argon matrices as well as in supersonic expansions. For the 1:1 pyrrole-N_2 interaction two stable forms were reported: one with N_2 hydrogen bonded to the NH unit and the other with N_2 situated above the ring plane (π-type complex). A small NH stretching downshift of 5 cm^{-1} was predicted for the hydrogen bonded complex whereas νNH mode appeared to be insensitive to complexation in the π-type complex [22].

Triazoles and their derivatives belong to one of the most important heterocyclic family. There is a wealth of literature on derivatives of 1,2,4-triazole which covers such subjects as crystal structure determination [40–42], theoretical and experimental vibrational characteristics of different triazole tautomers and conformers [43–53], photochemical transformations [54–63] and thermal decomposition processes [64–69].

In this work we present our results obtained for the complexes of the 1,2,4-triazole and 3-amino-1,2,4-triazole with dinitrogen isolated in solid argon. To our knowledge, there have been no matrix isolation studies on these systems. The experimental FTIR studies are supported by quantum chemical calculations at MP2 and B3LYPD3 with 6-311++G(2d,2p) basis set. The analysis of the results was focused on the types of interactions that appear in the studied systems as well as on the influence of the matrix environment on the spectroscopic properties of these weak complexes.

In line with the early work of Maier et al. [60] in current experiments one of three possible tautomers was detected for 1,2,4-triazole (TR) in argon matrices, namely *1H*-TR. It is worth mentioning that TR spectra are characterized by doublets or multiplets in many spectral regions originating from different matrix sites. Especially the NH stretching vibration in azoles turned out to be particularly sensitive to even small changes in the matrix environment [51,61,70–72]. A full analysis of the spectra of TR isolated in argon matrices has not been published. Maier et al. [60] presented 1600–400 cm^{-1} region of the azole compared to its calculated spectra. In turn, Pagacz-Kostrzewa et al. [67] presented assignment of the most intense 1,2,4-triazole monomer bands observed in an argon matrix. Matrix isolation spectrum of monomeric 3-amino-1,2,4-triazole (AT) in solid argon is well known and interpreted. Both *1H* and *2H* tautomers were detected in AT/Ar matrices with an abundance close to that predicted for the gas phase population (80 % and 20 %, respectively) [52].

2. Experimental

2.1. Computational methods

All calculations were carried out using the Gaussian 16 program package [73]. The structures of the monomers and the 1,2,4-triazole and 3-amino-1,2,4-triazole complexes with N_2 were optimized at the MP2 [74–77] and B3LYPD3 [78–82] levels of theory using the 6-311++G(2d,2p) [83,84] basis set. Optimization of the complexes was done with the Boys-Bernardi full counterpoise method by Dannenberg et al. [85,86]. The interaction energies were estimated by subtracting the energies of the isolated monomers with the frozen geometry from the energy of the complexes. Energies of the optimized structures at B3LYPD3/6-311++G(2d,2p) level were further refined by single-point calculations using CCSD(T) and MP4 methods. Wavenumbers were computed at harmonic approximations in the aim to confirm that the obtained structures correspond to the minima on their potential energy surfaces and to follow the changes in vibrational spectra upon complex formation. The topological analysis of electron density (AIM) [87,88] was performed at the MP2/6-311++G(2d,2p) level using AIM studio program (Version 19.10.12, Professional) [89].

2.2. Matrix isolation FTIR studies

1,2,4-triazole (98 %) and 3-amino-1,2,4-triazole (97 %) were purchased from Sigma-Aldrich and Fluka, respectively, and N_2 (6.0) and Ar (5.0) from Messer. Both triazoles were pumped before use to get rid of volatile impurities. A crystalline sample of the 1,2,4-triazole (TR) or 3-amino-1,2,4-triazole (AT) was allowed to sublimate at 290 K or 333 K, respectively from a small glass oven placed inside the vacuum chamber of the cryostat. The vapor of either TR or AT was mixed with argon or with the N_2/Ar mixture and deposited onto a cold CsI window kept at 15 K. The gaseous N_2/Ar mixtures were prepared by mixing appropriate amounts of dinitrogen with argon in a stainless steel vacuum line to obtain N_2/Ar concentration of 1/1000, 1/2000 or 1/4000. An accurate concentration of the triazoles in matrices was not known, but optimizing of the matrix gas flow allowed to obtain conditions which helped to minimalize aggregation of TR and AT. Pressure of the gas mixtures and the deposition rates were controlled by piezo transducers (model 902B, MKS Instruments) installed in the deposition line. FTIR spectra were recorded between 4000 and 400 cm^{-1} by means of Nicolet iS50 spectrometer with resolution of 0.5 cm^{-1} as the average of 128 scans. Liquid N_2 cooled MCT detector was used. Low temperature was obtained by means of a closed cycle helium refrigerator (APD Cryogenics). The temperature was measured by a silicon diode sensor working with a

digital controller (Scientific Instruments, model 9700).

3. Results and discussion

3.1. Quantum chemical calculations

Out of three tautomeric structures of TR the most stable *1H* form (hereafter referred to as TR) is present in low temperature matrices in accordance with the theoretically estimated abundance of 100 % [67]. In turn, the two most abundant tautomers of AT, *1H*-AT and *2H*-AT (hereafter referred to as 1AT and 2AT), have their population equal approximately to 80 % and 20 %, respectively [52,62]. Therefore, the interaction of TR and both 1AT and 2AT with dinitrogen will be considered as these complexes are likely to appear in argon matrices.

3.1.1. Structure and energetics of the TR complexes with N_2 of the 1:1 stoichiometry

At both levels of theory-five minima were found for the 1:1 complex formed between TR and dinitrogen. Cartesian coordinates of the optimized species are provided in Table S1 in the Supplementary material. There are no significant differences between the B3LYPD3 and MP2 calculated geometrical parameters. Fig. 1 presents the MP2 optimized geometries of the 1:1 complexes together with the adopted atom numbering. Table 1, however, contains their MP2 calculated values of intermolecular distances and angles as well as the values of two topological AIM parameters: the electron density ρ(r) and its Laplacian $\nabla^2\rho(r)$ at the critical points. The positions of the critical points derived from AIM calculations are also depicted in Fig. 1. These parameters may provide important information regarding the types of non-covalent interaction in the studied complexes. It happens that the AIM method does not result to bond paths with chemical meaning especially when the bond path charts are very complex [90,91]. However, it is very useful to indicate how the complex is built up, showing how the nitrogen molecule is connected with the triazole subunit.

Several types of complexes have been found on the TR···N_2 potential energy surface. There is one hydrogen-bonded structure TR-N1 which comprises a non-linear N-H···N bridge with the N-H···N angle of 131.2° (DFT) and 132.9° (MP2). This structure is planar and according to the AIM studies is characterized by the values of both the electron density ρ(r) and its Laplacian $\nabla^2\rho(r)$ at the BCP in the proper range for hydrogen bonding of 0.0002–0.0340 au and 0.024–0.139 au, respectively [92,93]. It is worth noting that the N-H···N hydrogen bond is the only intermolecular interaction found in TR-N1. The C-H···N interaction was detected, based on the AIM results, in TR-N3, TR-N4 and TR-N5 complexes. The C-H···N bonds are strongly bent, which is often the case with weak hydrogen bonds [67,94], with the CHN angles within the 112.9–114.8° (DFT) and the 112.5–114.1° (MP2) ranges. In addition to the C-H···N bond, the van der Waals interaction was detected in all three structures

Table 1
Interatomic distances (Å), angles (degree) and electron density parameters of the intermolecular bond critical points BCP (au) and ring critical points RCP (au) of the TR complexes with N_2 (1:1) computed at the MP2/6-311++G(2d,2p) level.

Complex TR···N_2	Intermolecular parameters[a]			AIM parameters		
	Interatomic distances		Angle	BCP	ρ(r)	$\nabla^2\rho(r)$
	H···Y	X···Y	X–H···Y			
TR-N1	2.420	3.191	132.9	H8···N9	0.0091	0.0355
TR-N2		3.263		N1···N9	0.0053	0.0185
		3.374		C3···N10	0.0045	0.0162
RCP1 (N4-C3-N10-N9-N1-C5)				(6 at.)	0.0039	0.0160
RCP2 (N2-N1-N9-N10-C3)				(5 at.)	0.0042	0.0172
TR-N3		3.334		N4···N9	0.0043	0.0150
	2.829	3.389	112.5	H6···N9	0.0047	0.0177
RCP (N4-C5-H6-N9)				(4 at.)	0.0040	0.0171
TR-N4		3.330		N4···N9	0.0042	0.0147
	2.894	3.459	113.0	H7···N9	0.0041	0.0156
RCP (H7-C3-N4-N9)				(4 at.)	0.0036	0.0160
TR-N5		3.328		N2···N9	0.0048	0.0170
	2.920	3.498	114.1	H7···N9	0.0045	0.0173
RCP (H7-C3-N2-N9)				(4 at.)	0.0041	0.0178

[a] X: N or C, Y: N.

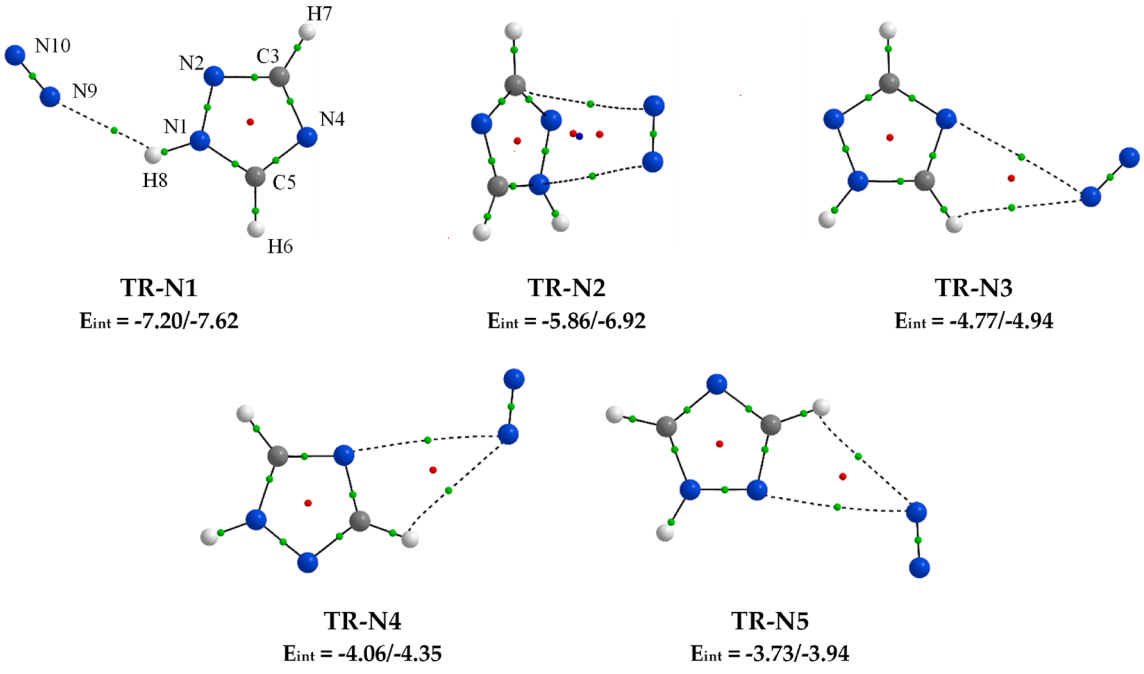

Fig. 1. The MP2 optimized structures of TR complexes with N_2 of the 1:1 stoichiometry. Positions of the bond (3,-1), ring (3,+1) and cage (3,+3) critical points derived from AIM calculations are shown by small green, red and dark blue dots, respectively. Below the structures, the values of the interaction energies (kJ/mol) calculated at B3LYPD3/MP2 levels are given.

formed between N atom of the nitrogen molecule, already involved in the C-H···N bonding and one of the N atoms of the triazole ring. One structure with the N_2 molecule interacting with the aromatic ring was also optimized (TR-N2). The N_2 molecule in this complex is located above the ring lying on the plane containing one of the C-H bonds and bisecting the ring in the middle of the N1-C5 bond. The AIM bond paths in this π complex connect the N atoms of the N_2 molecule with one nitrogen atom and one carbon atom of the azole ring.

The Laplacian of the (3,-1) bond critical points is positive for all discussed structures, indicating a minimum charge density along the bond, as is characteristic of closed-shell interactions (hydrogen bond or van der Waals). In turn, different number and location of the bond critical points reflect the appearance and distribution of the (3,+1) ring critical points and the (3,+3) cage critical point appearing due to the complex formation. There is one RCP in all C-H···N hydrogen bonded structures and their presence may be considered as a guarantee of the consistent topology [52]. Topology found in the π-bonded complex (TR-N2) is particularly interesting. In addition to two BCPs, two ring and one cage critical points occur in this structure.

Table 2 shows the values of relative energies and interaction energies of the TR complexes with dinitrogen of 1:1 stoichiometry using MP2 and B3LYPD3 methods as well as results of CCSD(T) and MP4 single point calculations at the B3LYPD3 optimized geometry. The interaction energy trend is independent on the method used. All TR complexes appeared to be weak with the values in the range of 7.20–3.73 kJ mol^{-1} (B3LYPD3) and 7.62–3.94 kJ mol^{-1} (MP2).

3.1.2. Structure and energetics of the AT complexes with N_2 of the 1:1 stoichiometry

Five and four minima were found on the potential energy surfaces of the 1AT···N_2 and 2AT···N_2 complexes, respectively (see Fig. 2 and Fig. S1). For both AT tautomers similar geometries of the complexes were optimized. Cartesian coordinates of the optimized species are presented in Table S2 in the Supplementary material. There is one structure with the N_2 molecule interacting with the aromatic ring (1AT-N2 and 2AT-N2) and one comprising the C-H···N interaction (1AT-N5, 2AT-N5). Two types of the N-H···N hydrogen bonds were found in the studied complexes involving either N-H group (1AT-N1 and 2AT-N1) or NH_2 group (1AT-N3, 1AT-N4 and 2AT-N3). Due to steric effects the 1AT-N4 form does not have its counterpart for the 2AT. The N_2 moiety in most structures containing an N-H···N bond is co-planar with the azole ring, except for 1AT-N4.

The AIM electron density parameters for 1AT complexes with dinitrogen and interatomic geometric parameters are gathered in Table 3 while those for 2AT complexes are presented in Table S3 in the Supplementary material. The obtained results indicate that the N-H···N hydrogen bond formed by pyrrolic N-H group of AT is stronger than those formed by amino group, although the former bridge is stronger bent.

Table 4 presents the energetic parameters of the 1AT complexes with N_2 of the 1:1 stoichiometry and those for 2AT are shown in Table S4 in the Supplementary material. The interaction energy and relative energy orders are the same for both computational methods used. Generally, all N_2 complexes are weak with the interaction energy E_{int} comparable to that obtained for TR complexes in the range of 7.03–4.77 kJ mol^{-1} (B3LYPD3) and 8.08–4.94 kJ mol^{-1} (MP2) for 1AT and 7.66–4.06 kJ mol^{-1} (B3LYPD3) and 8.88–4.35 kJ mol^{-1} (MP2) for 2AT. Additionally, single point calculations were performed at CCSD(T) and MP4 with the geometry optimized at B3LYPD3. Interestingly, application of the more advanced methods for the energy estimation led to an important change in the stability of the two most stable structures. It appeared that the N-H···N hydrogen bonded structure 1AT-N1 is more stable than that bound by N···π interaction, which turns out to be in agreement with the experimental findings (see section 3.2.3).

Table 2
Relative energies ΔE (kJ/mol) and BSSE corrected interaction energies E_{int} (kJ/mol) of TR complexes with N_2 calculated at B3LYPD3 and MP2 levels. CCSD(T) and MP4 results are from single point calculations performed at the B3LYPD3 geometries.

	Method	Complex				
		TR-N1	TR-N2	TR-N3	TR-N4	TR-N5
ΔE	B3LYPD3	0.00	1.33	2.39	3.11	3.46
	MP2	0.00	0.68	2.68	3.27	3.66
	CCSD(T)	0.00	2.05	2.37	2.99	3.31
	MP4	0.00	1.71	2.48	3.07	3.46
E_{int}	B3LYPD3	−7.20	−5.86	−4.77	−4.06	−3.73
	MP2	−7.62	−6.95	−4.94	−4.35	−3.94
	CCSD(T)	−6.57	−4.40	−4.10	−3.48	−3.14
	MP4	−7.12	−5.23	−4.52	−3.94	−3.52

3.1.3. Structure and energetics of the TR and 1AT complexes with N_2 of the 1:2 stoichiometry

Structures of TR and 1AT complexes with dinitrogen of the stoichiometry 1:2 were also optimized. Five minima were found at MP2 and B3LYPD3 levels of theory on the potential energy surface of both TR and 1AT interacting with two nitrogen molecules. Their structures are presented in Fig. S2 in the Supplementary material. The calculated values of intermolecular distances and angles together with the values of two AIM parameters ρ(r) and $\nabla^2\rho(r)$ at the critical points are gathered in Tables S5 and S6 and their energetics is shown in Tables S7 and S8 in the Supplementary material. As can be seen in Fig. S2, the same types of interaction as for the 1:1 complexes are present in the 1:2 aggregates. There are the N-H···N, C-H···N hydrogen bonds and N···N or N···π-type interactions. The TR complexes with two nitrogen molecules are characterized by interaction energy E_{int} in the range of 14.86–12.02 kJ mol^{-1} (MP2) and 13.36–10.80 kJ mol^{-1} (B3LYPD3) (Table S7) while those of AT in the range of 15.83–11.74 kJ mol^{-1} (MP2) and 14.32–11.72 kJ mol^{-1} (B3LYPD3) (Table S8).

3.1.4. Structure of TR dimer and complexes with N_2 of the 2:1 stoichiometry

As mentioned in Experimental section a small amount of the dimer species was detected in the matrices containing TR. For this reason, calculations at the B3LYPD3/6-311++G(2d,2p) level were performed for the dimer and the TR complexes with dinitrogen of the 2:1 stoichiometry. Their structures and energetics as well as wavenumber shifts for the NH stretching modes are presented in Figs S3 and S4 and Tables S9 and S10.

3.2. Matrix isolation infrared spectra

Before experiments on TR and AT complexes with dinitrogen were performed, blank experiments were conducted for TR/Ar and AT/Ar matrices. The obtained infrared spectra are in agreement with those previously reported [52,67].

3.2.1. Complexes of TR with dinitrogen isolated in argon matrices

Fig. 3 shows selected ranges of the spectrum of the TR/N_2/Ar matrix obtained after co-deposition of the TR vapor with N_2/Ar = 1/2000 gas mixture compared to the TR/Ar spectrum. The B3LYPD3/6-311++G(2d,2p) theoretical stick spectra of TR and one of its complexes with N_2: TR-N1 are presented at the bottom of the figure. As shown, when TR and N_2/Ar mixtures were co-deposited at 15 K (10 K for measurements) new absorptions, usually in the form of multiplets, were observed as compared with the TR/Ar spectrum. The figure also presents behavior of these bands upon 10 min annealing at 32 K and cooling down to 10 K. The selected experimental wavenumber shifts compared to those computed for different 1:1 TR complexes with N_2 are presented in Table 5. In turn, selected band positions and their intensities calculated for these species are gathered in Table S11 in the Supplementary material.

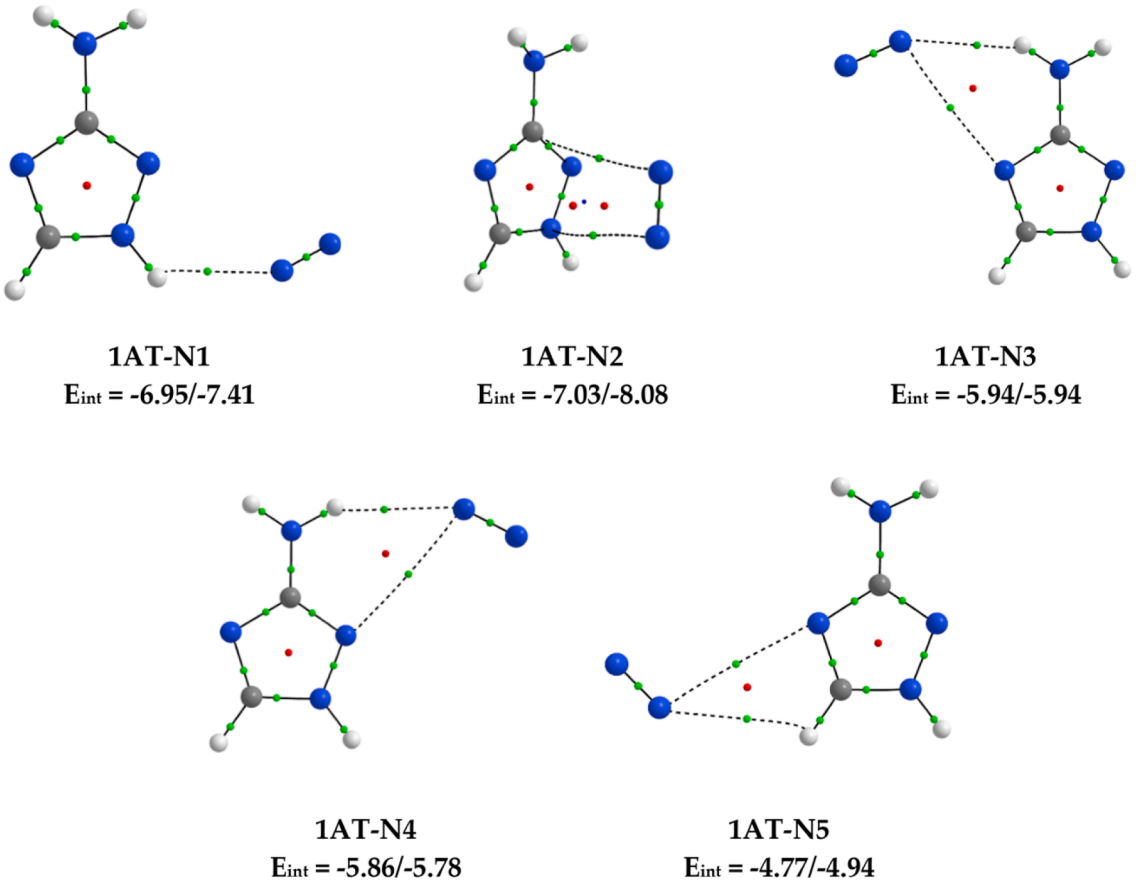

Fig. 2. The MP2 optimized structures of the 1:1 complexes of 1AT with N_2. The positions of the bond (3,-1), ring (3,+1) and cage (3,+3) critical points derived from AIM calculations are shown by small green, red and dark blue dots, respectively. Below the structures, the values of the interaction energies (kJ/mol) calculated at B3LYPD3/MP2 levels are given.

Table 3
Interatomic distances (Å), angles (degree) and electron density parameters of the intermolecular bond critical points BCP (au) and ring critical points RCP (au) of the 1AT complexes with N_2 (1:1) computed at the MP2/6-311++G(2d,2p) level.

Complex 1AT···N_2	Intermolecular parameters[a]			AIM parameters		
	Interatomic distances		Angle	BCP	ρ(r)	$\nabla^2\rho(r)$
	H···Y	X···Y	X–H···Y			
1AT-N1	2.468	3.194	128.6	H10···N11	0.0083	0.0324
1AT-N2		3.322		N1···N11	0.0049	0.0175
		3.214		C3···N12	0.0058	0.0212
RCP1 (N1-N2-C3-N12-N11)				(5 at.)	0.0044	0.0187
RCP2 (N1-C5-N4-C3-N12-N11)				(6 at.)	0.0042	0.0175
1AT-N3	2.546	3.468	152.0	H8···N11	0.0066	0.0249
		3.376		N4···N11	0.0043	0.0135
RCP (H8-N6-C3-N4-N11)				(5 at.)	0.0035	0.0139
1AT-N4	2.552	3.470	151.3	H7···N11	0.0066	0.0247
		3.368		N2···N11	0.0042	0.0134
RCP (H7-N6-C3-N2-N11)				(5 at.)	0.0034	0.0137
1AT-N5	2.829	3.355	112.5	H9···N11	0.0047	0.0177
		3.329		N4···N11	0.0043	0.0151
RCP (H9-C5-N4-N11)				(4 at.)	0.0040	0.0171

[a] X: N or C, Y: N.

In the NH stretching range a triplet absorption, below the TR monomer value, is observed with the sub-maxima at 3490.5, 3486.5 and 3483.0 cm^{-1}. The intensity ratio of these components is constant in the

Table 4
Relative energies ΔE (kJ/mol) and BSSE corrected interaction energies E_{int} (kJ/mol) of 1AT complexes with N_2 calculated at B3LYPD3 and MP2 levels. CCSD(T) and MP4 results are from single point calculations performed at the B3LYPD3 geometries.

	Method	Complex				
		1AT-N1	1AT-N2	1AT-N3	1AT-N4	1AT-N5
ΔE	B3LYPD3	0.11	0.00	1.10	1.19	2.28
	MP2	0.66	0.00	2.17	2.36	3.16
	CCSD(T)	0.00	1.12	1.30	1.41	2.19
	MP4	0.00	0.58	1.37	1.53	2.32
E_{int}	B3LYPD3	−6.95	−7.03	−5.94	−5.86	−4.77
	MP2	−7.41	−8.08	−5.94	−5.78	−4.94
	CCSD(T)	−6.36	−5.11	−5.11	−4.98	−4.10
	MP4	−6.91	−6.15	−5.57	−5.44	−4.52

spectra obtained for both N_2/Ar concentrations used (see Fig. S5), indicating that this absorption originates from the 1:1 TR···N_2 complexes. The wavenumber shifts relative to the corresponding mode in monomeric TR (an average of the 3498.0/3496.0 cm^{-1} doublet) are equal to −6.5, −9.5 and −14.0 cm^{-1}, respectively. Inspection of Table 5 revealed that among five stable TR···N_2 (1:1) complexes only one, TR-N1, has the predicted νNH shift matching to the experimental values. Other structures are characterized by clearly smaller wavenumber shift values between 0 and −2 cm^{-1}.

The bands appearing in the NH region are accompanied by new features in the vicinity of other TR bands. In the 1550–900 cm^{-1} range there are bands attributed to the in-plane ring stretching modes (νCN and νNN) and in-plane δCH and δNH deformations. Below 900 cm^{-1}

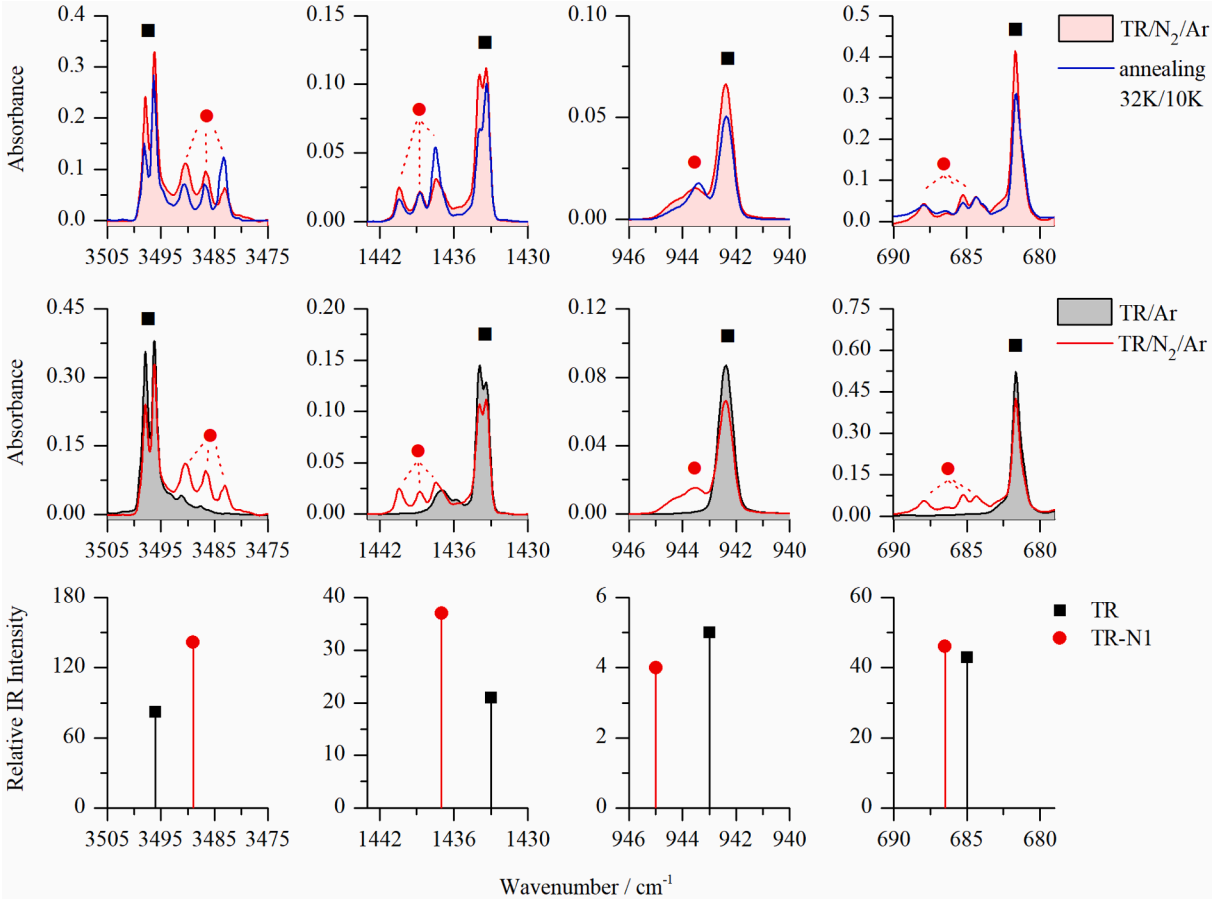

Fig. 3. Selected regions in the spectra of matrices: TR/Ar (black trace), TR co-deposited with N_2/Ar = 1/2000 (red trace), the latter spectrum after matrix annealing at 32 K/10 K (blue trace) and stick spectra of TR monomer and TR-N1 complex calculated at B3LYPD3/6-311++G(2d,2p) level.

Table 5
Selected wavenumber shifts calculated for the 1:1 TR complexes with N_2 using the MP2 and B3LYPD3 methods with the 6-311++G(2d,2p) basis set compared to the experimental results.

Calculated shifts[a]										Mode[b]	Experimental shifts[c]	
B3LYPD3					MP2							
N1	N2	N3	N4	N5	N1	N2	N3	N4	N5			
−7	0	0	0	0	−11	−2	0	0	0	νNH	−6.5, −9.5, −14.0	(3497.0)
+4	+1	+2	+1	0	+3	0	+1	+1	0	νCN + δNH + δCH + δ_{ring}	+6.5, +4.5, +3.5	(1434.0)
−1	−1	0	0	0	+2	+1	+1	+1	+1	νCN + δ_{ring} + δCH	+4.0, +2.5, +1.5	(1353.5)
+2	+1	+1	0	+1	+1	0	0	−1	0	νNN + δCH + δ_{ring}	+6.0, +3.0	(1047.0)
+2	+1	+1	0	0	+2	0	+1	0	0	δ_{ring} + δCH	+1.0	(942.5)
+1	0	0	+1	0	+8	0	0	+1	0	γNCN_{ring}	+6.0, +4.5, +3.5, +2.5	(682.0)
+31	+5	+2	+1	−1	+25	+3	+2	0	−2	γNH + τ_{ring}	+31.0, +23.5, +20.0, +17.5	(550.0)

[a] N1, N2, N3, N4 and N5 denote TR-N1, TR-N2, TR-N3, TR-N4 and TR-N5, respectively.
[b] Modes assignment are those shown in reference [67]. Abbreviations: ν – bond stretching, δ – bending, deformation in plane, γ – out-of-plane bending.
[c] The corresponding TR monomer band positions are shown in brackets. In the most cases an average of two band components due to multiple matrix sites were taken.

bands originating from the out-of-plane deformation modes of TR ring and NH group are observed. Additional bands appearing due to the TR···N_2 complex formation are usually blue-shifted compared to the corresponding monomer modes. As shown in Table 5, the observed shifts of several wavenumbers match, with some exceptions, relatively well to those predicted theoretically for the TR-N1 complex. The analysis was difficult due to the fact that the wavenumber shifts obtained on the basis of the two calculation methods used differ in some cases. However, it can be concluded on the basis of the obtained results that the TR-N1 structure is present in the studied matrices. Similarly to the νNH stretching mode, a multiplet structure of absorption is present, although not so pronounced, in other spectral regions. For instance, a triplet observed in the 1442–1436 cm^{-1} range due to deformation mode of the triazole ring have separation of 2.0 and 1.0 cm^{-1}. In turn, the out-of-plane deformation of the ring (690–683 cm^{-1}) is split to four components separated by 1.5, 1.0 and 1.0 cm^{-1}.

As demonstrated in Fig. 3, annealing of the deposited matrices at 32 K/10 K leads to changes in the component intensities of the absorptions attributed to the TR-N1 complex. It can be noticed that one of the subbands in the multiplets increases its intensity at the expense of the other components. Such behavior under the influence of annealing with simultaneous low splitting values within the multiplets indicates the

presence of multiple trapping sites in the matrix which can slightly differently perturb the structure of the complex. Position of the 3483.0 cm^{-1} component of the trio observed in the νNH range fits also to that predicted theoretically for one of the TR complexes of the 2:1 stoichiometry (DN3). However, as shown in Table S10, its population in the studied matrices is expected to be negligible.

It is worth noting that the presence of other 1:1 TR···N_2 structures in the matrix, characterized by similar energy values (see Table 2), cannot be completely excluded. It is due to the fact that the wavenumber shifts predicted in the calculations are in many cases very small or zero and can be overlap by TR monomer bands. In turn, under the conditions of the experiment with 0.05 % or less of N_2 in the sample, the 1:2 complexes are not very probable to be formed in the deposited matrices. Selected band positions and their intensities calculated for TR complexes with N_2 of the 1:2 stoichiometry are presented Table S12 in the Supplementary material.

3.2.2. *Complexes of AT with dinitrogen isolated in argon matrices*

Fig. 4 shows selected ranges of the AT/N_2/Ar matrix spectrum obtained after co-deposition of the AT vapor with N_2/Ar = 1/1000. When dinitrogen is present in an argon matrix, in addition to the AT molecules, a number of new bands grow in the spectra, all situated in the vicinity of the AT monomer bands. Taking into account the population of AT tautomers (*ca.* 80 % and 20 %, respectively) [52,62] one may expect both 1AT and 2AT complexes with dinitrogen to be present in the studied matrix although the amount of the latter species should be much smaller.

The best clue for determining the structure of the 1AT complex with N_2 can be obtained in the NH stretching region. The observed wavenumber shift for this vibration best matches the calculated value for 1AT-N1 structure in which the NH group of the ring interacts with the nitrogen molecule. Wavenumber shifts for other modes predicted theoretically for this structure are also in good agreement with the experimental ones. An appropriate comparison of the selected experimental shifts with the calculated values for five 1AT···N_2 geometries is shown in Table 6. As in the case of complexes with TR, the presence of other AT···N_2 structures in the matrix, characterized by similar energy values (see Table 4), cannot be completely ruled out. The predicted wavenumber values for these species are in many cases very small or zero and can be overlap by AT monomer bands.

Interaction of dinitrogen with the less abundant 2AT tautomer could also be detected in the AT/N_2/Ar matrices. However, due to a small amount of 2AT species only a broadening of several monomeric bands was observed, as shown in Fig. S7 in the Supplementary material. Yet it was not possible to conclude on the exact geometry of the 2AT···N_2 complex based on these changes. Table S13 in the Supplementary material presents the experimental shifts compared to the calculated ones for all the possible structures.

Contrary to the situation described for the TR complexes with N_2, in the case of AT all bands of the complex appear in the form of singlets. A slight increase of the 1:1 complex band is observed upon annealing of the matrices and a weak shoulder at 3494 cm^{-1}, observed in the spectra at higher N_2/Ar concentration used, increases in intensity forming a weak band (see Fig. S7 in the Supplementary material). The latter peak is tentatively assigned to 1AT complex with dinitrogen of the 1:2 stoichiometry.

Analyzing the obtained results for the two structurally similar complexes TR-N1 and 1AT-N1 a question arises why multiple trapping sites are observed only in the spectra of the former complex. The observed differences may occur due to the presence of the amino group in 1AT, which acts as an "anchor", stiffening the system and reducing the susceptibility of vibrations in the 1AT-N1 complex to environmental changes. To obtain a full explanation of the observed disparity calculations with the help of molecular dynamics methods would be useful, which are however beyond the scope of this paper.

4. Conclusions

The results presented in this paper using FTIR spectroscopy coupled with matrix isolation technique and quantum chemical calculations showed that simple triazoles such as 1,2,4-triazole and 3-amino-1,2,4-triazole are capable of forming various types of complexes with a nitrogen molecule. Although the values of the interaction energy are similar for different types of complexes bound by hydrogen bonding or by the van der Waals interaction, one type of the 1:1 complex was detected in the argon matrix for both studied systems. Comparison of the

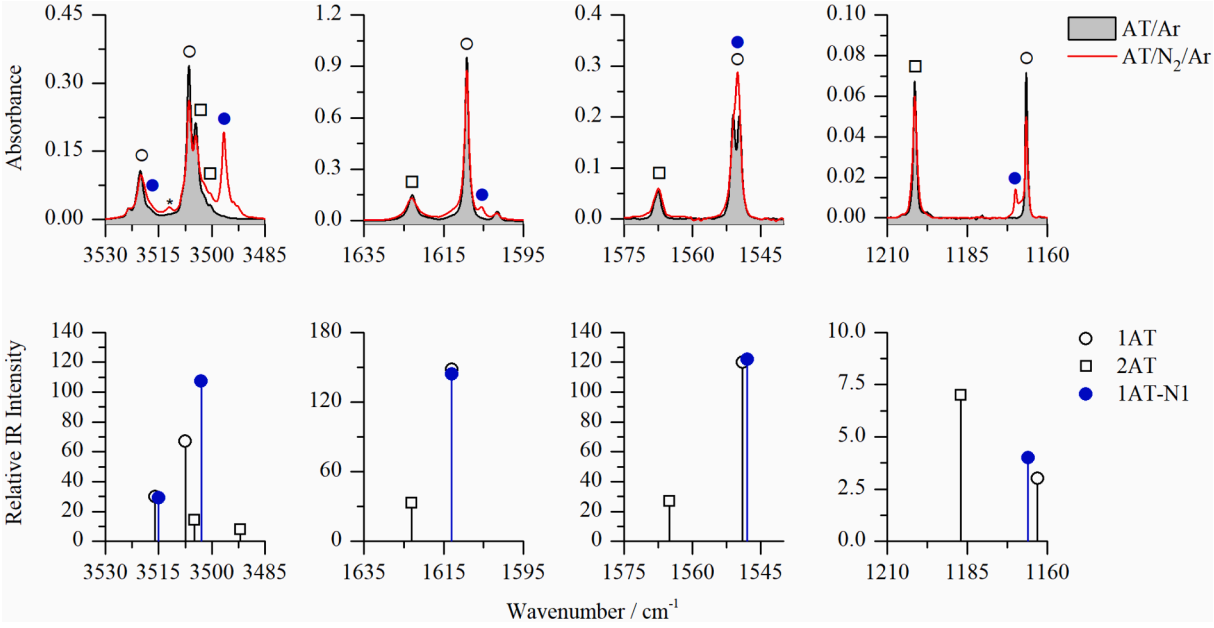

Fig. 4. Selected regions in the spectra of matrices: AT/Ar (black trace), AT co-deposited with N_2/Ar = 1/1000 (red trace) and stick spectra of AT monomers and 1AT-N1 complex calculated at B3LYPD3/6-311++G(2d,2p) level. A weak band at 3512 cm^{-1} marked with an asterisk which disappears upon annealing is tentatively assigned to non-near-neighbor AT···N_2 interaction.

Table 6
Selected wavenumber shifts calculated for the 1:1 complexes of 1AT with N_2 using the MP2 and B3LYPD3 methods with the 6-311++G(2d,2p) basis set compared to the experimental results.

Calculated shifts[a]										Mode[b]	Experimental shifts[c]	
B3LYPD3					MP2							
N1	N2	N3	N4	N5	N1	N2	N3	N4	N5			
−1	−2	+1	+2	−1	−3	−3	−4	−1	−2	$\nu_{as}NH_2$	−2.0sh	(3520.0)
−5	0	+1	+1	+1	−9	−2	+1	+1	0	νNH	−10.0	(3506.5)
0	−1	+2	+3	0	−3	−3	−3	−1	−3	ν_sNH_2	−1.0sh	(3425.0)
0	+1	+4	+4	0	−1	0	+4	+3	0	δNH_2	−3.5	(1609.0)
−1	−1	0	0	−1	−1	−1	0	0	−1	νCN_{ring}	+/- 0.5[d]	(1551.0, 1550.0)
+3	−1	0	−1	0	+3	1	+1	+1	+1	$\nu CN_{ring} + \delta NH$	+4.5	(1444.5)
+4	0	+1	0	+1	+2	0	0	0	0	$\nu CN_{ring} + \nu NN_{ring}$	+3.5	(1166.5)
0	0	−1	0	0	+1	0	+1	0	0	$\delta NNC_{ring} + \delta NCN_{ring}$	+1.5	(973.5)
+7	0	0	0	+2	+7	2	+4	+2	+1	γNCN_{ring}	+7.5	(645.0)
+36	+6	−2	−5	+2	+31	3	−1	−4	+3	γNH	+29.0	(477.0)
+3	+9	+7	+6	+2	+5	2	+3	+2	+2	γNH_2	+1.0sh	(434.5)

[a] N1, N2, N3, N4 and N5 denote 1AT-N1, 1AT-N2, 1AT-N3, 1AT-N4 and 1AT-N5, respectively.
[b] Modes assignment are those shown in reference [52]. Abbreviations: ν – bond stretching, δ – bending, deformation in plane, γ – out-of-plane bending.
[c] The corresponding AT monomer band positions are shown in brackets.
[d] A new band due to the 1AT-N1 complex appears between two AT monomer bands originating from the site effect.

infrared wavenumber shifts predicted theoretically for different types of complexes with those observed experimentally made it possible to identify the N-H···N hydrogen bonded structures (TR-N1 and 1AT-N1) in solid argon at low temperature. The hydrogen bond is formed in both cases between NH group of the triazole ring with one of the nitrogen atoms of the N_2 molecule. Interestingly, although both complexes are structurally similar, the results obtained for TR-N1 indicate a greater influence of the matrix on the vibrations of this complex. It is manifested by the presence of multiplets in many regions of the TR-N1/Ar spectrum, while in the case of 1AT-N1 single bands are observed.

CRediT authorship contribution statement

K. Mucha: Conceptualization, Investigation, Visualization, Writing – original draft. **M. Pagacz-Kostrzewa:** Investigation, Visualization, Writing – review & editing. **J. Krupa:** Investigation, Visualization, Formal analysis. **M. Wierzejewska:** Conceptualization, Writing – original draft, Supervision.

Declaration of Competing Interest

The authors declare that they have no known competing financial interests or personal relationships that could have appeared to influence the work reported in this paper.

Data availability

Data will be made available on request.

Acknowledgments

Allocation of computer time from the Wrocław Centre for Networking and Supercomputing (Wroclaw, Poland) is gratefully acknowledged.

The authors thank Jan Lundell (Department of Chemistry, University of Jyväskylä, Finland) and Robert Wieczorek (Faculty of Chemistry, University of Wrocław, Poland) for fruitful discussions.

Appendix A. Supplementary data

Supplementary data to this article can be found online at https://doi.org/10.1016/j.saa.2022.121901.

References

[1] L. Andrews, B.J. Kelsall, R.T. Arlinghaus, FTIR observation of the N_2···HF complex in solid argon, J. Chem. Phys. 79 (1983) 2488–2490, https://doi.org/10.1063/1.446093.
[2] L. Andrews, S.R. Davis, FTIR observation of N≡N stretching fundamentals in hydrogen-bonded complexes in solid argon, J. Chem. Phys. 83 (1985) 4983–4989, https://doi.org/10.1063/1.449763.
[3] A.J. Barnes, H.E. Hallam, G.F. Scrimshaw, Infra-red cryogenic studies. Part 3. –Hydrogen halides in doped argon matrices, Trans. Faraday Soc. 65 (1969) 3172–3178, https://doi.org/10.1039/TF9696503172.
[4] S. Coussan, A. Loutellier, J.P. Perchard, S. Racine, Y. Boutellier, Spectroscopic study of the tunneling dynamics in N_2-water observed in the O-D stretch region, J. Mol. Struct. 471 (1998) 37–47, https://doi.org/10.1063/5.0071732.
[5] S. Hirabayashi, K. Ohno, H. Abe, K.M.T. Yamada, Infrared spectra of the water-nitrogen complexes $(H_2O)_2$–$(N_2)_n$ (n=1–4) in argon matrices, J. Chem. Phys. 122 (2005), https://doi.org/10.1063/1.1901660, 194506/1-194506/6.
[6] J. Murto, M. Ovaska, Matrix infrared study of the specific interactions between methanol and nitrogen, and methanol and carbon monoxide, Spectrochim. Acta 39 (1983) 149–152, https://doi.org/10.1016/0584-8539(83)80072-5.
[7] S. Oswald, M. Wallrabe, M.A. Suhm, Cooperativity in Alcohol−Nitrogen Complexes: Understanding Cryomatrices through Slit Jet Expansions, J. Phys. Chem. A 121 (2017) 3411–3422.
[8] J. Lundell, M. Räsänen, Z. Latajka, Matrix isolation FTIR and ab initio study of complexes between formic acid and nitrogen, Chem. Phys. 189 (1994) 245–260, https://doi.org/10.1016/0301-0104(94)00226-6.
[9] K. Marushkevich, M. Räsänen, L. Khriachtchev, Interaction of Formic Acid with Nitrogen: Stabilization of the Higher-Energy Conformer, J. Phys. Chem. A 114 (2010) 10584–10589, https://doi.org/10.1021/jp105044r.
[10] Z. Mielke, Z. Latajka, J. Kołodziej, K.G. Tokhadze, Matrix Infrared Spectra and ab Initio Calculations of the Nitrous Acid Complexes with N_2 and CO, J. Phys. Chem. 100 (1996) 11610–11615, https://doi.org/10.1021/jp960452r.
[11] A.J. Barnes, E. Lasson, C.J. Nielsen, Molecular complexes of nitric acid with N_2, CO and NO studied by matrix isolation IR spectroscopy, J. Chem. Soc., Faraday Trans. 91 (1995) 3111–3116.
[12] M. Wierzejewska Hnat, Z. Latajka, Z. Mielke, H. Ratajczak, Theoretical and Infrared Matrix Isolation Studies of CF_3COOH-N_2 System, J. Mol. Struct. 129 (1985) 229–235, https://doi.org/10.1016/0022-2860(85)80166-6.
[13] A. Givan, A. Loewenschuss, C.J. Nielsen, IR spectrum of molecular complexes of sulfuric acid with N_2 and NO trapped in solid argon, Phys. Chem. Chem. Phys. 1 (1999) 37–43.
[14] M. Wierzejewska, R. Wieczorek, Infrared matrix isolation and ab initio studies on isothiocyanic acid HNCS and its complexes with nitrogen and xenon, Chem. Phys. 287 (2003) 169–181, https://doi.org/10.1016/S0301-0104(02)00989-8.
[15] J. Krupa, M. Wierzejewska, J. Lundell, Matrix isolation FTIR and theoretical study of weakly bound complexes of isocyanic acid with nitrogen, Molecules 27 (2022), https://doi.org/10.3390/molecules27020495, 495/1-495/16.
[16] B. Golec, J. Grzegorzek, Z. Mielke, Complexation of formaldoxime and acetaldoxime with nitrogen, Chem. Phys. 353 (2008) 13–18, https://doi.org/10.1016/j.chemphys.2008.07.020.
[17] M. Sałdyka, Z. Mielke, The interaction of formohydroxamic acid with nitrogen: FTIR matrix isolation and ab initio studies, J. Mol. Struct. 708 (2004) 183–188, https://doi.org/10.1016/j.molstruc.2004.05.020.
[18] M. Sałdyka, Z. Mielke, K. Mierzwicki, S. Coussan, P. Roubin, CH stretching vibration of N-methylformamide as a sensitive probe of its complexation: infrared matrix isolation and computational study, Phys. Chem. Chem. Phys. 13 (2011) 13992–14002, https://doi.org/10.1039/C1CP20743A.

[19] I. Kosendiak, J.M.E. Ahokas, J. Krupa, J. Lundell, M. Wierzejewska, Complexes of glycolic acid with nitrogen isolated in argon matrices. I. Structures and thermal effects, Molecules 24 (2019) 3262/1-3262/13. 10.3390/molecules24183262.

[20] J.M.E. Ahokas, I. Kosendiak, J. Krupa, M. Wierzejewska, J. Lundell, Raman spectroscopy of glycolic acid complexes with N_2, J. Mol. Struct. 1183 (2019) 367–372, https://doi.org/10.1016/j.molstruc.2019.01.080.

[21] Q. Cao, N. Andrijchenko, A.-E. Ahola, A. Domanskaya, M. Räsänen, A. Ermilov, A. Nemukhin, L. Khriachtchev, Interaction of phenol with xenon and nitrogen: Spectroscopic and computational characterization, J. Chem. Phys. 137 (2012), https://doi.org/10.1063/1.4754435, 134305/1-134305/11.

[22] S. Oswald, M.A. Suhm, S. Coussan, Incremental NH stretching downshift through stepwise nitrogen complexation of pyrrole: a combined jet expansion and matrix isolation study, Phys. Chem. Chem. Phys. 21 (2019) 1277–1284, https://doi.org/10.1039/c8cp07053a.

[23] M. Sałdyka, Z. Mielke, K. Haupa, Structural and spectroscopic characterization of DMF complexes with nitrogen, carbon dioxide, ammonia and water. Infrared matrix isolation and theoretical studies, Spectrochim. Acta A 190 (2018) 423–432, https://doi.org/10.1016/j.saa.2017.09.046.

[24] S. Oswald, S. Coussan, Chloroform–nitrogen aggregates: Upshifted CH and downshifted CCl stretching vibrations observed by matrix isolation and jet expansion infrared spectroscopy, Fiz. Nizk. Temp. 45 (2019) 750–759, https://doi.org/10.1063/1.5103257.

[25] P. Banerjee, T. Chakraborty, Confinement effects on C-H and C–F stretching vibrational frequencies of difluoromethane in cold inert gas matrixes: a combined infrared spectroscopy and electronic structure theory study, Eur. Phys. J. D 75 (2021), https://doi.org/10.1140/epjd/s10053-021-00142-3, 131/1-131/14.

[26] L. Khriachtchev, S. Tapio, M. Räsänen, A. Domanskaya, A. Lignell, HY···N_2 and HXeY···N_2 complexes in solid xenon (Y=Cl and Br): Unexpected suppression of the complex formation for deposition at higher temperature, J. Chem. Phys. 133 (2010), https://doi.org/10.1063/1.3472976, 084309/1-084309/7.

[27] A. Lignell, L. Khriachtchev, M. Pettersson, M. Räsänen, Interaction of rare-gas-containing molecules with nitrogen: Matrix-isolation and ab initio study of HArF···N_2, HKrF···N_2, and HKrCl···N_2 complexes, J. Chem. Phys. 118 (2003) 11120–11128, https://doi.org/10.1063/1.1575198.

[28] A. Lignell, L. Khriachtchev, H. Lignell, M. Räsänen, Protons solvated in noble-gas matrices: Interaction with nitrogen, Phys. Chem. Chem. Phys. 8 (2006) 2457–2463, https://doi.org/10.1039/b603822k.

[29] A.V. Lalov, S.E. Boganov, V.I. Faustov, M.P. Egorov, O.M. Nefedov, Experimental and quantum-chemical study of complexation of carbene analogs with dinitrogen. Direct IR-spectroscopic observation of $Cl_2Si{\bullet}N_2$ complexes in low-temperature argon-nitrogen matrices, Russ. Chem. Bull., Int. Ed. 52 (2003) 526–538, https://doi.org/10.1023/a:1023973815486.

[30] G. Maier, H.P. Reisenauer, J. Glatthaar, R. Zetzmann, Complex of Silylene with Nitrogen: A Combined Matrix-Spectroscopic and Density Functional Theory Study, Chem. Asian. J. 1–2 (2006) 195–202, https://doi.org/10.1002/asia.200600089.

[31] J.A.G. Castaño, A. Fantoni, R.M. Romano, Matrix-isolation FTIR study of carbon dioxide: Reinvestigation of the CO_2 dimer and CO_2···N_2 complex, J. Mol. Struct. 881 (2008) 68–75, https://doi.org/10.1016/j.molstruc.2007.08.035.

[32] R. Nowak, J.A. Menapace, E.R. Bernstein, Benzene clustered with N_2, CO_2, and CO: Energy levels, vibrational structure, and nucleation, J. Chem. Phys. 89 (1988) 1309–1321, https://doi.org/10.1063/1.455182.

[33] P. Hobza, O. Bludský, H.L. Selzle, E.W. Schlag, Ground state potential surface for van der Waals complexes: Ab initio second-order Möller-Plesset study on benzene···N_2 van der Waals molecule, J. Chem. Phys. 98 (1993) 6223–6226, https://doi.org/10.1063/1.464815.

[34] Y. Hu, W. Lu, S. Yang, Resonant two-photon ionization spectra of the van der Waals complexes: C_6H_5X···N_2 (X=F, Cl, Br), J. Chem. Phys. 105 (1996) 5305–5312, https://doi.org/10.1063/1.472408.

[35] T.A. Wesolowski, O. Parisel, Y. Ellinger, J. Weber, Comparative Study of Benzene···X (X = O_2, N_2, CO) Complexes Using Density Functional Theory: The Importance of an Accurate Exchange-Correlation Energy Density at High Reduced Density Gradients, J. Phys. Chem. A 101 (1997) 7818–7825, https://doi.org/10.1021/jp970586k.

[36] D.M. Chapman, K. Müller-Dethlefs, J.B. Peel, A comparison of hydrogen-bonded and van der Waals isomers of phenol···nitrogen and phenol···carbon monoxide: An ab initio study, J. Chem. Phys. 111 (1999) 1955–1963, https://doi.org/10.1063/1.479508.

[37] H.M. Jaeger, H.F. Schaefer III, C.E. Dykstra, The N_2-benzene tethered top, J. Mol. Struct. THEOCHEM 895 (2009) 168–171, https://doi.org/10.1016/j.theochem.2008.11.025.

[38] R. Knochenmuss, R.K. Sinha, S. Leutwyler, Intermolecular dissociation energies of dispersively bound complexes of aromatics with noble gases and nitrogen, J. Chem. Phys. 148 (2018), https://doi.org/10.1063/1.5019432, 134302/1-134302/13.

[39] R. Kanakaraju, P. Kolandaivel, Post Hartree-Fock and DFT Studies on Pyrrole···Nitrogen and Pyrrole···Carbon Monoxide Molecules, Int. J. Mol. Sci. 3 (2002) 777–789, https://doi.org/10.3390/i3070777.

[40] A.S. Lyakhov, A.N. Vorobiov, P.N. Gaponik, L.S. Ivashkevich, V.E. Matulis, O. A. Ivashkevich, Acta Cryst. C 59 (2003), https://doi.org/10.1107/S0108270103024442 o690-o693.

[41] L.-H. Jia, Z.-L. Liu, W. Liu, Acta Cryst. E 63 (2007), o2766, https://doi.org/10.1107/S1600536807020272.

[42] V. Arjunan, S. Thirunarayanan, M.K. Marchewka, S. Mohan, Crystal structure, vibrational spectra and DFT studies of hydrogen bonded 1,2,4 triazolium hydrogenselenate, J. Mol. Struct. 1145 (2017) 211–221, https://doi.org/10.1016/j.molstruc.2017.05.107.

[43] D.C. Sorescu, C.M. Bennett, D.L. Thompson, Theoretical Studies of the Structure, Tautomerism, and Vibrational Spectra of 3-Amino-5-nitro-1,2,4-triazole, J. Phys. A 102 (1998) 10348–10357, https://doi.org/10.1021/jp9824712.

[44] J.-L.-M. Abboud, C. Foces-Foces, R. Notario, R.E. Trifonov, A.P. Volovodenko, V. A. Ostrovskii, I. Alkorta, J. Elguero, Basicity of N-H- and N-Methyl-1,2,3-triazoles in the Gas Phase, in Solution, and in the Solid State - an Experimental and Theoretical Study, Eur. J. Org. Chem. (2001) 3013–3024, https://doi.org/10.1002/1099-0690(200108)2001:16<3013::AID-EJOC3013>3.0.CO;2-Y.

[45] W.P. Oziminski, J.C. Dobrowolski, A.P. Mazurek, DFT studies on tautomerism of C5-substituted 1,2,4-triazoles, J. Mol. Struct. (Theochem) 680 (1-3) (2004) 107–115.

[46] M.H. Palmer, D. Christen, An ab initio study of the structure, tautomerism and molecular properties of the C- and N-amino-1,2,4-triazoles, J. Mol. Struct. 705 (2004) 177–187, https://doi.org/10.1016/j.molstruc.2004.07.001.

[47] A.A. El-Azhary, H.U. Suter, J. Kubelka, Experimental and Theoretical Investigation of the Geometry and Vibrational Frequencies of 1,2,3-Triazole, 1,2,4-Triazole, and Tetrazole Anions, J. Phys. Chem. A 102 (3) (1998) 620–629, https://doi.org/10.1021/jp9719568.

[48] V. Jimenez, J.B. Alderete, Complete basis set calculations on the tautomerism and protonation of triazoles and tetrazole, J. Mol. Struct. (Thoechem) 775 (2006) 1–7, https://doi.org/10.1016/j.theochem.2006.06.010.

[49] G. da Silva, E.E. Moore, J.W. Bozzelli, Quantum Chemical Study of the Structure and Thermochemistry of the Five-Membered Nitrogen-Containing Heterocycles and Their Anions and Radicals, J. Phys. Chem. A 110 (51) (2006) 13979–13988, https://doi.org/10.1021/jp065150w.

[50] V.E. Matulis, O.A. Ivashkevich, P.N. Gaponik, P.D. Elkind, G.T. Sukhanov, A. B. Bazyleva, D.H. Zaitsau, Theoretical study of gas-phase formation enthalpies and isomerism for 4(5)-nitro-1,2,3-triazole and its N-alkyl derivatives and experimental determination of formation enthalpy for 2-methyl-4-nitro-1,2,3-triazole, J. Mol. Struct. (Thoechem) 854 (2008) 18–25, https://doi.org/10.1016/j.theochem.2007.12.009.

[51] M. Pagacz-Kostrzewa, M. Sałdyka, M. Wierzejewska, D.M. Khomenko, R. O. Doroschuk, Theoretical DFT and matrix isolation FTIR studies of 2-(1,2,4-triazolyl) phenol isomers, Chem. Phys. Lett. 657 (2016) 156–161, https://doi.org/10.1016/j.cplett.2016.06.005.

[52] M. Pagacz-Kostrzewa, R. Bronisz, M. Wierzejewska, Theoretical and matrix isolation FTIR studies of 3-amino-1,2,4-triazole and its isomers, Chem. Phys. Lett. 473 (2009) 238–246, https://doi.org/10.1016/j.cplett.2009.03.079.

[53] R.M. Balabin, Tautomeric equilibrium and hydrogen shifts in tetrazole and triazoles: Focal-point analysis and ab initio limit, J. Chem. Phys. 131 (2009), https://doi.org/10.1063/1.3249968, 154307/1-154307/8.

[54] F. Billes, H. Endredi, G. Keresztury, Vibrational spectroscopy of triazoles and tetrazole, J. Mol. Struct. (Theochem) 530 (2000) 183–200, https://doi.org/10.1016/S0166-1280(00)00340-7.

[55] V. Krishnakumar, R.J. Xavier, FT Raman and FT–IR spectral studies of 3-mercapto-1,2,4-triazole, Spectrochim. Acta, Part A 60 (2004) 709–714, https://doi.org/10.1016/S1386-1425(03)00281-6.

[56] S. Zaza, F. Guedira, S. Zaydoun, M. Saidi Idrissi, A. Lautie, F. Romain, Etude vibrationnelle du {1H}-5-amino-1, 2, 4-triazole et de son chlorhydrate. Site de protonation, Canadian J. Anal. Sci. Spectrosc. 49(1) (2004) 15–23.

[57] V. Krishnakumar, G. Keresztury, T. Sundius, R.J. Xavier, Hydrogen bonding and molecular vibrations of 3,5-diamino-1,2,4-triazole, Spectrochim. Acta, Part A 61 (2005) 261–267, https://doi.org/10.1016/j.saa.2004.03.039.

[58] S. Thomas, N. Biswas, S. Venkateswaran, S. Kapoor, R. D'Cunha, T. Mukherjee, Raman, infrared, SERS and DFT calculations of a triazole derivative (akacid), Chem. Phys. Lett. 402 (2005) 361–366, https://doi.org/10.1016/j.cplett.2004.12.064.

[59] M. Kiszka, I.R. Dunkin, J. Gebicki, H. Wang, J. Wirz, The photochemical transformation and tautomeric composition of matrix isolated benzotriazole, J. Chem. Soc., Perkin Trans. 2 (2000) 2420–2426, https://doi.org/10.1039/b006754g.

[60] G. Maier, J. Eckwert, A. Bothur, H.P. Reisenauer, C. Schmidt, Photochemical fragmentation of unsubstituted tetrazole, 1,2,3-triazole, and 1,2,4-triazole: first matrix-spectroscopic identification of nitrilimine HCNNH, Liebigs Ann. 7 (1996) 1041–1053, https://doi.org/10.1002/jlac.199619960704.

[61] M. Pagacz-Kostrzewa, M. Sałdyka, A. Bil, W. Gul, M. Wierzejewska, D. M. Khomenko, R.O. Doroschuk, Phototransformations of 2-(1,2,4-triazol-3-yl) benzoic acid in low temperature matrices, J. Phys. Chem. A 123 (2019) 841–850, https://doi.org/10.1021/acs.jpca.8b10762.

[62] M. Pagacz-Kostrzewa, A. Bil, M. Wierzejewska, UV-induced proton transfer in 3-amino-1,2,4-triazole, J. Photochem. Photobiol. A-Chem. 335 (2017) 124–129, https://doi.org/10.1016/j.jphotochem.2016.11.023.

[63] M. Pagacz-Kostrzewa, I.D. Reva, R. Bronisz, B.M. Giuliano, R. Fausto, M. Wierzejewska, Conformational behavior and tautomer selective photochemistry in low temperature matrices: the case of 5-(1H-tetrazol-1-yl)-1,2,4-triazole, J. Phys. Chem. A 115 (2011) 5693–5707, https://doi.org/10.1021/jp202925r.

[64] P.J. Sánchez-Soto, E. Morillo, J.L. Pérez-Rodríguez, C. Real, Thermoanalytical study of the pesticide 3-amino-1,2,4-triazole, J. Therm. Anal. 45 (1995) 1189–1197, https://doi.org/10.1007/bf02547493.

[65] J. Li, T.A. Litzinger, Thermal decomposition of 4-amino-1,2,4-triazolium nitrate under infrared laser heating, Thermochim. Acta 454 (2007) 116–127, https://doi.org/10.1016/j.tca.2007.01.013.

[66] M. Badea, R. Olar, D. Marinescu, G. Vasile, Thermal behavior of some new triazole derivative complexes, J. Therm. Anal. Calorim. 92 (2008) 209–214, https://doi.org/10.1007/s10973-007-8766-4.

[67] M. Pagacz-Kostrzewa, J. Krupa, W. Gul, M. Wierzejewska, FTIR matrix isolation studies of thermal decomposition of 1,2,4-triazolyl-3-carboxylic acid, J. Mol. Struct. 1209 (2020), https://doi.org/10.1016/j.molstruc.2020.127938, 127938/1-127938/7.
[68] C. Wentrup, Flash Vacuum Pyrolysis of Azides, Triazoles, and Tetrazoles, Chem. Rev. 117 (2017) 4562–4623, https://doi.org/10.1021/acs.chemrev.6b00738.
[69] D. Kvaskoff, P. Bednarek, L. George, S. Pankajakshan, C. Wentrup, Different behavior of nitrenes and carbenes on photolysis and thermolysis: Formation of azirine, ylidic cumulene, and cyclic ketenimine and the rearrangement of 6-phenanthridylcarbene to 9-phenanthrylnitrene, J. Org. Chem. 70 (20) (2005) 7947–7955, https://doi.org/10.1021/jo050898g.
[70] M. Pagacz-Kostrzewa, M. Sałdyka, W. Gul, M. Wierzejewska, D.M. Khomenko, R. O. Doroschuk, Infrared spectra and photochemistry of 2-(tetrazol-5-yl) benzoic acid isolated in nitrogen matrices, J. Photochem. Photobiol. A Chem. 371 (2019) 292–299, https://doi.org/10.1016/j.jphotochem.2018.11.031.
[71] C. Araujo-Andrade, I. Reva, R. Fausto, Tetrazole acetic acid: tautomers, conformers, and isomerization, J. Chem. Phys. 140 (2014), https://doi.org/10.1063/1.4864119, 064306/1-064306/14.
[72] A. Gomez-Zavaglia, I.D. Reva, L. Frija, M.L. Cristiano, R. Fausto, Photochemistry of 1-phenyl-tetrazolone isolated in solid argon, J. Photochem. Photobiol. A Chem. 179 (2006) 243–255, https://doi.org/10.1016/j.jphotochem.2005.08.021.
[73] Gaussian 16, Revision C.01, M.J. Frisch, G.W. Trucks, H.B. Schlegel, G.E. Scuseria, M.A. Robb, J.R. Cheeseman, G. Scalmani, V. Barone, G.A. Petersson, H. Nakatsuji, X. Li, M. Caricato, A.V. Marenich, J. Bloino, B.G. Janesko, R. Gomperts, B. Mennucci, H.P. Hratchian, J.V. Ortiz, A.F. Izmaylov, J.L. Sonnenberg, D. Williams-Young, F. Ding, F. Lipparini, F. Egidi, J. Goings, B. Peng, A. Petrone, T. Henderson, D. Ranasinghe, V.G. Zakrzewski, J. Gao, N. Rega, G. Zheng, W. Liang, M. Hada, M. Ehara, K. Toyota, R. Fukuda, J. Hasegawa, M. Ishida, T. Nakajima, Y. Honda, O. Kitao, H. Nakai, T. Vreven, K. Throssell, J.A. Montgomery, Jr., J.E. Peralta, F. Ogliaro, M.J. Bearpark, J.J. Heyd, E.N. Brothers, K.N. Kudin, V.N. Staroverov, T.A. Keith, R. Kobayashi, J. Normand, K. Raghavachari, A.P. Rendell, J.C. Burant, S.S. Iyengar, J. Tomasi, M. Cossi, J.M. Millam, M. Klene, C. Adamo, R. Cammi, J.W. Ochterski, R.L. Martin, K. Morokuma, O. Farkas, J.B. Foresman, D.J. Fox, Gaussian, Inc., Wallingford CT, 2016.
[74] M. Head-Gordon, J.A. Pople, M.J. Frisch, MP2 energy evaluation by direct methods, Chem. Phys. Lett. 153 (1988) 503–506, https://doi.org/10.1016/0009-2614(88)85250-3.
[75] M. Head-Gordon, T. Head-Gordon, Analytic MP2 Frequencies Without Fifth Order Storage: Theory and Application to Bifurcated Hydrogen Bonds in the Water Hexamer, Chem. Phys. Lett. 220 (1994) 122–128, https://doi.org/10.1016/0009-2614(94)00116-2.
[76] M.J. Frisch, M. Head-Gordon, J.A. Pople, Semi-direct algorithms for the MP2 energy and gradient, Chem. Phys. Lett. 166 (1990) 281–289, https://doi.org/10.1016/0009-2614(90)80030-H.
[77] S. Sæbø, J. Almlöf, Avoiding the integral storage bottleneck in LCAO calculations of electron correlation, Chem. Phys. Lett. 154 (1989) 83–89, https://doi.org/10.1016/0009-2614(89)87442-1.
[78] A.D. Becke, Density-functional exchange-energy approximation with correct asymptotic-behavior, Phys. Rev. A 38 (1988) 3098–3100, https://doi.org/10.1103/PhysRevA.38.3098.
[79] A.D. Becke, Density-functional thermochemistry. III. The role of exact exchange, J. Chem. Phys. 98 (1993) 5648–5652, https://doi.org/10.1063/1.464913.
[80] C. Lee, W. Yang, R.G. Parr, Development of the Colle-Salvetti correlation-energy formula into a functional of the electron density, Phys. Rev. B 37 (1988) 785–789, https://doi.org/10.1103/PhysRevB.37.785.
[81] S. Grimme, J. Antony, S. Ehrlich, H. Krieg, A consistent and accurate ab initio parameterization of density functional dispersion correction (DFT-D) for the 94 elements H-Pu, J. Chem. Phys. 132 (2010), https://doi.org/10.1063/1.3382344, 154104/1-154104/19.
[82] S. Grimme, S. Ehrlich, L. Goerigk, Effect of the damping function in dispersion corrected density functional theory, J. Comp. Chem. 32 (2011) 1456–1465, https://doi.org/10.1002/jcc.21759.
[83] A.D. McLean, G.S. Chandler, Contracted Gaussian-basis sets for molecular calculations. I. Second row atoms, Z=11-18, J. Chem. Phys. 72 (1980) 5639–5648, https://doi.org/10.1063/1.438980.
[84] K. Raghavachari, J.S. Binkley, R. Seeger, J.A. Pople, Self-Consistent Molecular Orbital Methods. XX. Basis set for correlated wave functions, J. Chem. Phys. 72 (1980) 650–654, https://doi.org/10.1063/1.438955.
[85] S.F. Boys, F. Bernardi, Calculation of small molecular interactions by differences of separate total energies. Some procedures with reduced errors, Mol. Phys. 19 (1970) 553–566, https://doi.org/10.1080/00268977000101561.
[86] S. Simon, M. Duran, J.J. Dannenberg, How does basis set superposition error change the potential surfaces for hydrogen-bonded dimers? J. Chem. Phys. 105 (1996) 11024–11031, https://doi.org/10.1063/1.472902.
[87] R.F.W. Bader, Atoms In Molecules, A Quantum Theory, Oxford University Press, Oxford, UK, 1990.
[88] R.F.W. Bader, A Quantum Theory of Molecular Structure and its Applications, Chem. Rev. 91 (1991) 893–928, https://doi.org/10.1021/cr00005a013.
[89] AIMAll (Version 19.10.12), T.A. Keith, TK Gristmill Software, Overland Park KS, USA, 2019 (aim.tkgristmill.com).
[90] E. Cerpa, A. Krapp, A. Vela, G. Merino, The implications of symmetry of the external potential on bond paths, Chem. Eur. J. 14 (2008) 10232–10234, https://doi.org/10.1002/chem.200800934.
[91] J.R. Lane, J. Contreras-Garcia, J.-P. Piquemal, B.J. Miller, H.G. Kjaergaard, Are bond critical points really critical for hydrogen bonding? J. Chem. Theor. Comput. 9 (2013) 3263–3266, https://doi.org/10.1021/ct400420r.
[92] U. Koch, P.L.A. Popelier, Characterization of C-H-O hydrogen bonds on the basis of the charge density, J. Phys. Chem. 99 (1995) 9747–9754, https://doi.org/10.1021/j100024a016.
[93] S.J. Grabowski, What Is the Covalency of Hydrogen Bonding? Chem. Rev. 111 (2011) 2597–2625, https://doi.org/10.1021/cr800346f.
[94] G.R. Desiraju, T. Steiner, The Weak Hydrogen Bond in Structural Chemistry and Biology, Oxford University Press Inc., New York, 1999.